

Research Article

Tracking Control of Wind Energy Conversion System in Green Crop Producing Bases

Jianhua Liu

Bureau of Education Department of Yueyang, Yueyang, Hunan 410114, P.R. China

Abstract: The tracking control of directly driven wind energy conversion system in green crop producing bases in green crop producing bases is studied in this study. The design procedure in this study aims at designing stable neural network slide mode controllers that guarantee the existence of the system poles in some predefined zone and wind speed precise tracking. More significantly, the speed tracking control problems are reduced to Lyapunov stability problem. In this way, by solving the stability Lyapunov functions, the feedback gains which guarantee global asymptotic stability and desired speed tracking performance are determined. The results are applied to a wind turbine generator systems and numerical simulation showing the feasibility of the proposed method.

Keywords: Green crop producing bases, lyapunov, tracking control, wind energy conversion

INTRODUCTION

Among the main research subjects in the wind turbine domain, the control of Wind Energy Conversion System (WECS) in green crop producing bases is considered an interesting application area for control theory and engineering (Ekren and Ekren, 2010; Hazra and Sensarma, 2010; Bouscayrol *et al.*, 2009). The control strategies must cope with the exacting characteristics presented by WECS such as the nonlinear behavior of the system, the random variability of the wind and external perturbations. Djohra *et al.* (2010) model and simulate a wind turbine and an induction generator system as an electricity source in the southern parts of Algeria and the obtained results have then been validated by the HOMER software confirming the effectiveness of the developed program. Jordi *et al.* (2011a, 2011b) analyze and compares different control tuning strategies for a variable speed wind energy conversion system in green crop producing bases based on a Permanent-Magnet Synchronous Generator (PMSG) and the aerodynamics of the wind turbine and a PMSG have been modeled. De Battista *et al.* (2000) study the grid interconnection of a Permanent Magnet Synchronous Generator (PMSG)-based wind turbine with harmonics and reactive power compensation capability at the Point of Common Coupling (PCC) and the proposed system consists of two back-to-back connected converters with a common dc-link.

The speed tracking of directly driven WECS with intelligent slide mode control method is studied in particular in this study. The design procedure in this study aims at designing stable neural network slide mode controller that guarantee the existence of the system poles in some predefined zone and wind speed

precise tracking. More significantly, the controller design problem is reduced to Lyapunov stability problem. In this way, by solving the stability Lyapunov function, the feedback gains which guarantee global asymptotic stability and desired speed tracking performance are determined.

WIND TURBINE GENERATOR SYSTEM MODEL

In the first, we analyze the particular aerodynamic characteristics of windmills. Here the horizontal-axis type is considered. The output mechanical power available from a wind turbine is:

$$P = 0.5 \rho C_p (V_\omega)^3 A \quad (1)$$

where, ρ is the air density, A is the area swept by the blades, V_ω is the wind speed, C_p is the power coefficient and a nonlinear function of the parameter λ is given as $\lambda = \omega R / V_\omega$, where R is the radius of the turbine and ω is the rotational speed. C_p is approximated as $C_p = \alpha \lambda + \beta \lambda^2 + \gamma \lambda^3$ usually, where α , β and γ are design parameters for a given turbine. The torque developed by the windmill is:

$$T_t = 0.5 \left(\frac{C_p}{\lambda} \right) (V_m)^2 \pi R^2 \quad (2)$$

The torque developed by the generator/Kramer drive combination is:

$$T_g = \frac{3V^2 s R_{eq}}{\Omega_2 [(sR_s + R_{eq})^2 + (s\omega_s L_{ls} + s\omega_s L_{lr})^2]} \quad (3)$$

where,

$$R_{eq} = \frac{s[n_2^2 s R_b + (n_1 |\cos(\alpha)|)^2 R_s - n_1 |\cos(\alpha)|]}{(n_2 s)^2 - (n_1 |\cos(\alpha)|)^2},$$

$$R_b = R_r + 0.55 R_f,$$

$$\Gamma = 2n_2^2 R_b s R_s + (n_2 s R_s)^2 + n_2^2 (s \omega_s L_{ls} + s \omega_s L_{lr})^2 \quad (4)$$

With n_1 transformation rate between rotor and stator wounds; n_2 transformation rate between the Kramer Drive and the AC line; R_r, R_s, R_f Rotor, stator and dc link resistance respectively; L_{ls} stator dispersion inductance; L_{lr} rotor dispersion inductance; α firing angle; ω_s synchronous pulsation; Ω_s synchronous mechanic rotational speed.

With the above mentioned content, ignoring torsion in the shaft, generator electric dynamics and other higher order effects, the approximate system dynamic model is:

$$J\dot{\omega} + \rho(x, \theta) = T_1(\omega, V_\omega) - T_g(\omega, V_\omega) \quad (5)$$

where, J is the total moment of inertia, $\rho(x, \theta)$ means the dynamical uncertainties whose time-varying uncertain parameter θ appears nonlinearly, x represents any component of the system state, i.e., $x = [\omega, \dot{\omega}]^T$. We focus on the case where the uncertainties admit a general multiplicative form, i.e., $\rho(x, \theta) = g(x, \theta)h(x, \theta)$, where the functions $\rho(x, \theta), h(x, \theta)$ are assumed nonlinear and Lipschitzian in θ , $\theta = [\theta_1, \dots, \theta_p]^T \in R^p$.

In the following, $\|\cdot\|$ denotes the standard Euclidean norm. Note that all smooth or convex or concave functions satisfy the following Lipschitz condition.

Definition: Functions $g(x, \theta): R^r \times R^p \rightarrow (R^m)^T$ and $h(x, \theta): R^r \times R^p \rightarrow (R^m)^T$ are said to be Lipschitzian in θ if there exist continuous functions $L_j(x) \geq 0, l_j(x) \geq 0$ such that for $\forall(x, \theta, \bar{\theta})$, the following inequalities:

$$\|g(x, \theta) - g(x, \bar{\theta})\| \leq \sum_{j=1}^p L_j(x) |\theta_j - \bar{\theta}_j|$$

$$\|h(x, \theta) - h(x, \bar{\theta})\| \leq \sum_{j=1}^p l_j(x) |\theta_j - \bar{\theta}_j| \quad (6)$$

hold true.

Regarding (2) and (3), system model becomes:

$$\dot{\omega} = \frac{1}{J} \left(0.5 \rho \left(\frac{C_p}{\lambda} \right) (V_\omega)^2 \pi R^2 - \frac{3V^2 s R_{eq}}{\Omega_s [\Omega_s [(sR_s + R_{eq})^2 + (s\omega_s L_{ls} + s\omega_s L_{lr})^2]]} \right) \quad (7)$$

where R_{eq} depends nonlinearly on the control action $\cos(\alpha)$ according to (4), C_p, λ and V_ω also depend on ω in a nonlinear way. The shape of the generator curves allows a simple linearization on the expression for:

$$T_g = -k_1 \omega + k_2 \cos(\alpha) \quad (8)$$

As it can be verified, the proposed approximation is good in the required operation zone. The resulting expression for the whole system is then:

$$\dot{\omega} = \frac{0.5}{J} \rho \left(\frac{C_p}{\lambda} \right) (V_\omega)^2 \pi R^2 - k_1 \omega + k_2 \cos(\alpha) - \rho(x, \theta) \quad (9)$$

Which has the standard normal form:

$$\dot{\omega} + k_1 \omega = k_2 u + f(x) - \rho(x, \theta) \quad (10)$$

Here, $f(\cdot)$ is a nonlinear function, b is a constant and $u = \cos(\alpha)$.

Assumption 1: The reference output r is piecewise continuously time varying and uniformly bounded and there is a known positive constant m_r such that $|r| < m_r$.

Lemma 1: Given Lipschitzian functions $g(x, \theta), h(x, \theta)$, let $L(x)$ and $l(x)$ be defined as:

$$L(x) := \max_{j=1,2,\dots,p} L_j(x), \quad l(x) := \max_{j=1,2,\dots,p} l_j(x)$$

Then, for $\theta \in R_+^p$, the following inequalities:

$$e(t)g(x, \theta)h(x, \theta) \leq e(t)g(x, 0)h(x, 0) + |e(t)| \cdot \left\{ L l(x) \left(\sum_{j=1}^p \theta_j \right)^2 + \|h(x, 0)\| L(x) + \|g(x, 0)\| l(x) \left(\sum_{j=1}^p \theta_j \right) \right\}, \quad (11)$$

hold true for any $e(t) \in R$.

NEURAL NETWORK SILDE MODE CONTROL FOR SPEED TRACKING

Neural network approximate theory: In the field of control engineering, neural network is often used to approximate a given nonlinear function up to a small error tolerance. The function approximation problem can be stated formally as follows.

Definition 1: Given that $f(y): R^n \rightarrow R^m$ is a continuous function defined on the set $y \in R^n$ and $\hat{f}(W, y): R^{l \times m} \times R^n \rightarrow R^m$ is an approximating function that depends continuously on the parameter matrix W and y , the approximation problem is to determine the optimal parameter W^* such that, for some metric (or distance function) d :

$$d(f(W^*, y), f(y)) \leq \varepsilon, \quad (12)$$

For an acceptable small ε .

In this study, Gaussian Radial Basis Function (RBF) neural network is considered. It is a particular network architecture which uses 1 numbers of Gaussian function of the form:

$$\Theta(y) = \exp\left(-\frac{(y-\mu)^2}{\sigma^2}\right) \quad (13)$$

where, $\mu = R^i$ is the center vector and $\sigma^2 = R$ is the variance. At the input layer, the input space is divided into grids with a basis function at each node defining a receptive field in R^n . The output of the network $\hat{f}(W, y)$ is given by:

$$\hat{f}(W, y) = W^T \Theta(y) \quad (14)$$

where, $\Theta(y) = [\Theta_1(y)\Theta_2(y)\dots\Theta_l(y)]^T$ is the vector of basis function. Note that only the connections from the hidden layer to the output are weighted.

In succeeding sections, we will use the aforesaid RBF networks to approximate nonlinear function $f(\cdot)$, namely:

$$f = W^T \Theta(y) + \varepsilon \quad (15)$$

where, ε is network approximation difference which can be arbitrary small and in our paper we assume the difference satisfy $|\varepsilon| < k$, $\Theta(y)$ is network activation function and y is network input.

Neural network slide mode method: The tracking error of WT speed is defined as $e = \omega - r$. Introduce a new variable:

$$e_c = e - \frac{1}{\sqrt{2}} c_e \quad (16)$$

where,

$$c(e) = \begin{cases} b + \sqrt{r^2 - (e - \varepsilon)^2}, & ((\sqrt{2} - 1)/2)\varepsilon \leq e \leq \varepsilon \\ \sqrt{2}e, & \|e\| \leq ((\sqrt{2} - 1)/2)\varepsilon \\ -b - \sqrt{r^2 - (e + \varepsilon)^2}, & \varepsilon \leq e \leq ((\sqrt{2} - 1)/2)\varepsilon \\ \varepsilon \operatorname{sgn}(e), & \|e\| > \varepsilon \end{cases} \quad (17)$$

with $r = (\sqrt{2} - 1)\varepsilon$, $b = (2 - \sqrt{2})\varepsilon$, for $\varepsilon > 0$.

It is standard to show that such $c(e)$ is continuously differentiable in time. Regarding (17), the dynamics of system (10) in terms of the modified "velocity error" is expressed by:

$$\dot{e}_c + k_1 e_c = k_2 u + f(x) - \rho(x, \theta) \quad (18)$$

Consider a quadratic Lyapunov function candidate:

$$V_1(t) = \frac{1}{2} e_c^T(t) e_c(t) \quad (19)$$

Using the Gaussian RBF neural network approximation for $f(x)$ and setting $\tau = k_2 u$, the time derivative can be written as:

$$\dot{V}_1(t) = e_c^T (\tau - W^T \Theta - \rho(x, \theta)) = e_c^T (\tau - W^T \Theta) - e_c \rho(x, \theta) \quad (20)$$

where, the notation on t are neglected for simplicity. In view of relation (11), it follows that:

$$\begin{aligned} \dot{V}_1(t) &= e_c^T (\tau - W^T \Theta) + (e_c g(x, 0) h(x, 0)) \\ &+ |e_c| \left\{ L(x) l(x) \left(\sum_{j=1}^n \theta_j \right)^2 + \|h(x, 0)\| L(x) + \|g(x)\| l(x) \cdot \sum_{j=1}^n \theta_j \right\} \end{aligned} \quad (21)$$

With the definitions:

$$\begin{aligned} K(x) &= [\omega_1 \quad \omega_2] = [L(x) l(x) \quad \|h(x)\| L(x) + \|g(x)\| l(x)] \\ \beta &= [\beta_1 \quad \beta_2] = \left[\left(\sum_{j=1}^n \theta_j \right)^2 \quad \sum_{j=1}^n \theta_j \right], \quad \Phi(e, x) = \operatorname{sgn}(e) W(x), \end{aligned} \quad (22)$$

The inequality (21) can be rewritten as:

$$\dot{V}_1(t) = e_c^T (\tau - W^T \Theta) + s^T \rho(x, 0) + e_c^T \Phi(e_c, x) \beta, \quad (23)$$

where, $\tilde{\Theta} = \hat{\Theta} - \Theta$ and $\tilde{\beta} = \hat{\beta} - \beta$ are parameter errors and $K_D \in R$ is an arbitrary positive number. In order to derive update laws for the parameter estimates, we employ the following Lyapunov function:

$$V_c(t) = V_1(t) + \frac{1}{2} (\tilde{\Theta}^T \Gamma_\Theta^{-1} \tilde{\Theta} + \tilde{\beta}^T \Gamma_\beta^{-1} \tilde{\beta}) \quad (24)$$

It follows from (23) that:

$$\begin{aligned} \dot{V}_1(t) &\leq e_c^T (\tau - W^T \Theta) + e_c^T \rho(x, 0) \\ &+ e_c^T \Phi(e_c, x) \beta + \dot{\hat{\Theta}}^T \Gamma_\Theta^{-1} \tilde{\Theta} + \dot{\hat{\beta}}^T \Gamma_\beta^{-1} \tilde{\beta} \end{aligned}, \quad (25)$$

where, Φ is defined by formula (22).

Not that:

$$\begin{cases} e_c = 0, & |e_c| \leq ((\sqrt{2} - 1)/2)\varepsilon \\ e_c^2 \leq e_c e, \operatorname{sgn}(e) = \operatorname{sgn}(e_c) & |e_c| > ((\sqrt{2} - 1)/2)\varepsilon \end{cases} \quad (26)$$

Hence, introducing the saturated function:

$$\operatorname{sat}_\varepsilon(e) = \begin{cases} \frac{e}{((\sqrt{2} - 1)/2)\varepsilon}, & |e| \leq ((\sqrt{2} - 1)/2)\varepsilon \\ \operatorname{sgn}(e) & |e| > ((\sqrt{2} - 1)/2)\varepsilon \end{cases} \quad (27)$$

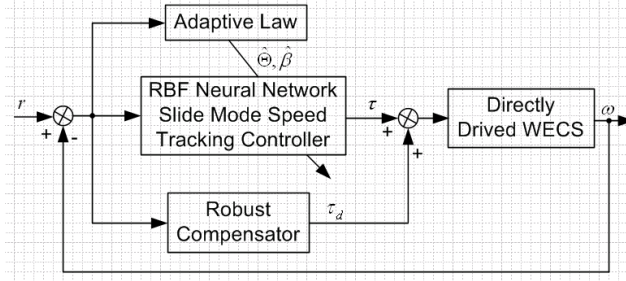


Fig. 1: Neural network slide mode speed tracking control system

Table 1: Parameters for the wind turbine and induction generator used for simulations

Parameter	Turbine		Parameter	Generator	
	Value	Units		Value	Units
ρ	1.204	Ns^2/m^4	R_f	0.2	Ω
R	0.95	M	R_s	0.3	Ω
J	0.312	Nm^2/red	R_r	0.3	Ω
α	-0.02		L_{ls}	1.2×10^{-3}	Hy
β	0.16		L_{lr}	0.65×10^{-3}	Hy
γ	-0.12		n_2	2	
			n_1	1	

And taking (25) and (26) into account, the following continuous control input:

$$\tau = -K_D e_\varepsilon + W^T \hat{\Theta} + k - \rho(x, 0) - \Phi_\varepsilon(e, x) \hat{\beta}, \quad (28)$$

Or:

$$u = \frac{1}{k_2} (-K_D e_\varepsilon + W^T \hat{\Theta} + k - \rho(x, 0) - \Phi_\varepsilon(e, x) \hat{\beta}) \quad (29)$$

With:

$$\Phi_\varepsilon(e, x) = \text{sat}_\varepsilon(e) W(x) \quad (30)$$

And the following update laws:

$$\dot{\hat{\Theta}} = -\Gamma_\Theta W^T e_\varepsilon, \quad \dot{\hat{\beta}} = -\Gamma_\beta K^T(x) |e_\varepsilon|, \quad (31)$$

Results in:

$$\dot{V}_1(t) \leq -e_\varepsilon^T K_D e_\varepsilon + e_\varepsilon^T [W^T \tilde{\Theta} - \Phi_\varepsilon(e, x)] \tilde{\beta}, \quad (32)$$

Yield:

$$\dot{V}_1(t) \leq -e_\varepsilon^T K_D e_\varepsilon \quad (33)$$

The last inequality implies that $V(t)$ is decreasing and thus is bounded by $V(0)$. Consequently, $e_s(t)$ and $\tilde{\alpha}(t)$ must be bounded quantities by virtue of definition (25). Given the boundedness of the reference trajectory γ , one has $\dot{e}_\varepsilon(t) \in L_\infty$ from the system dynamics (19).

Also, relation (34) gives $K_D \cdot \int_0^T |e(t)|^2 dt \leq V(0), \forall t > 0$ i.e., $e(t) \in L_2$. Applying Barbalats lemma yields $\lim_{t \rightarrow \infty} e_\varepsilon(t) = 0$, or equivalently, $\lim_{t \rightarrow \infty} e(t) \leq ((\sqrt{2}-1)/2)\varepsilon$, that is, the tracking error e converges to $((\sqrt{2}-1)/2)\varepsilon$ as $t \rightarrow \infty$. In this way, we sum up the following result.

Theorem 1: The adaptive controller defined by (17), (18) and (28)-(30) enable WECS system (10) to asymptotically tracking a desired wind speed r within a precision of $((\sqrt{2}-1)/2)\varepsilon$.

SIMULATION

In the following part, simulations are carried out using MATLAB 2006a to verify the performance of the neural network slide mode speed tracking controller. The overall system block diagram is depicted in Fig. 1 and the turbine and generator parameter values are given in Table 1. The adaptive weights are initialized on random values between -1 and 1 and the reference output is chosen as pulse wave. To quantify the control performance, the root-mean square average of tracking error (based on the L_2 norm of the tracking errors e) was used, which is given by:

$$L_2[e] = \sqrt{\frac{1}{T-t_0} \int_{t_0}^T e^T e dt} \quad (34)$$

where, T represents the total experimentation time and t_0 is the initial time of interest. The better performance is for the smaller L_2 norm.

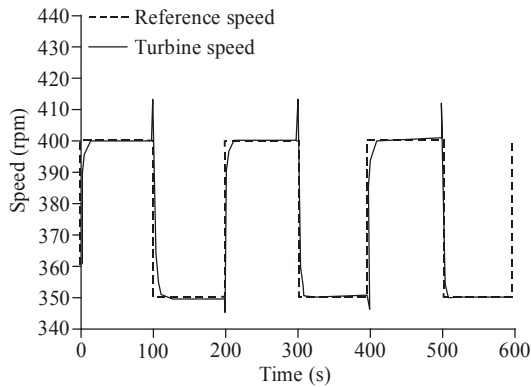


Fig. 2: Speed tracking control performance with sliding mode method in De Battista *et al.* (2000)

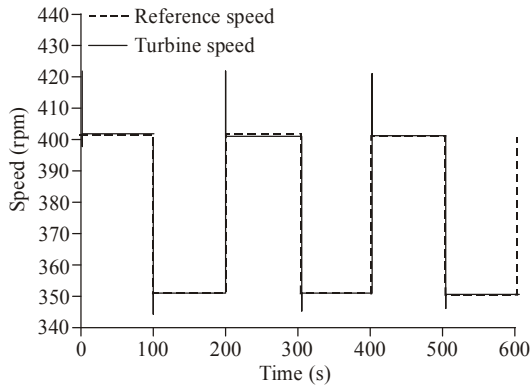


Fig. 3: Speed tracking control performance with proposed neural network slide mode method

The speed tracking performance of our method and are displayed in Fig. 2 and 3. A pseudoaleatory sequence of step-shaped wind gusts is applied to the system. It is clearly that from Fig. 3, with the neural network slide mode speed tracking controller, the resulting evolution of the closed loop converges rapidly to the desired optimal rotational speed with simple first-order dynamics. However, with the dynamical sliding mode power controller, there exists some obvious vibrations and deviations in the Fig. 2.

CONCLUSION

A neural network slide mode speed tracking control algorithm for directly driven WECS is presented in this study. The proposed intelligent robust controller guarantee global asymptotic stability of wind speed tracking control system and desired speed tracking performance with user specified dynamics.

The form of the network weight adaptation law for the neural network slide mode controller are derived from a Lyapunov stability theory. The numerical simulation shows that our control strategy owns the excellent performance in WECS than the existing result.

ACKNOWLEDGMENT

This study was supported by Key Laboratory Foundation for power technology of renewable energy sources of Hunan Province (2011KFJJ004), Postdoctoral Foundation of China (20110491241), National Natural Science Foundation of China (60835004, 41007601), Foundation of Hunan Province Science and Technology Department (2011RS4035), Research Foundation of Hunan Provincial Education Department (10C0356) and Graduate Innovation Foundation of Hunan Province (521298297[08]).

REFERENCES

- Bouscayrol, A., X. Guillaud, P. Delarue and B. Lemaire-Semail, 2009. Energetic macroscopic representation and inversion-based control illustrated on a wind-energy-conversion system using hardware-in-the-loop simulation. *IEEE T. Ind. Electron.*, 56(12): 4826-4835.
- De Battista, H., R.J. Mantz and C.F. Christiansen, 2000. Dynamical sliding mode power control of wind driven induction generators. *IEEE T. Energy Convers.*, 15(4): 451-457.
- Djohra, K., H. Mourad, B. Maiouf, H. Seddik and N. Said, 2010. Modeling and simulation of the fixed-speed WECS wind energy conversion system: Application to the Algerian Sahara area. *Energy*, 35(10): 4116-4125.
- Ekren, O. and Y.B. Ekren, 2010. Size optimization of a PV/Wind hybrid energy conversion system with battery storage using simulated annealing. *Appl. Energ.*, 87(2): 592-598.
- Hazra, S. and P.S. Sensarma, 2010. Self-excitation and control of an induction generator in a stand-alone wind energy conversion system. *IET Renew. Power Gen.*, 4(4): 383-393.
- Jordi, Z., P. Josep, A. Antoni, S. Cyril, R. Eider and C. Salvador, 2011a. Study and experimental verification of control tuning strategies in a variable speed wind energy conversion system. *Renew. Energ.*, 36: 1421-1430.
- Jordi, Z., P. Josep, A. Antoni, S. Cyril, R. Eider and C. Salvador, 2011b. *IET Power Electr.*, 4: 122.